

# 220 GHz Sparse Imaging with Multi-static Aperiodic Array

Shaoqing Hu<sup>a</sup>, Amir Masoud Molaei<sup>b</sup>, and Okan Yurduseven<sup>b</sup>

<sup>a</sup>Department of Electronic and Electrical Engineering, Brunel University London, Kingston Lane, London, United Kingdom

<sup>b</sup>School of Electronics, Electrical Engineering and Computer Science, Queen's University Belfast, University Road, Belfast, United Kingdom

## ABSTRACT

This paper proposes a simple design method for a multi-static aperiodic array to achieve 220 GHz sparse imaging, and a corresponding image reconstruction algorithm based on Fast Fourier Transform (FFT) and sparse data recovery. The proposed aperiodic sparse array originates from the linear sparse periodic array (SPA), it can further save the number of sampling data, transceivers and system cost compared to SPA imaging system. Low rank matrix recovery technique with principal component pursuit by alternating directions method (PCPADM) is used to recover the missing data caused by the sparse sampling. In order to achieve fast image reconstruction, FFT-based matched filtering method is used in which multistatic-to-monostatic conversion and interpolation are applied for data pre-processing. The proposed imaging scheme has been verified in experiments. An imaging resolution of 6 mm resolution is achieved at 1.4 m with 192 mm  $\times$  300 mm field of view, with a significantly reduced reconstruction time in comparison to the generalized synthetic aperture focusing technique (GSAFT).

**Keywords:** Aperiodic array, Fast Fourier Transform (FFT) matched filtering, generalized synthetic aperture focusing technique (GSAFT), low rank matrix recovery (LRMR), linear sparse periodic array (SPA), multi-static multiple-input and multiple-output (MIMO), millimeter-wave/THz imaging, synthetic aperture imaging, sparse imaging

## 1. INTRODUCTION

Imaging at millimetre-wave(mm-wave) and THz frequencies offers significant advantages for security/target detection, personnel screening and non-destructive testing due to its superiority on high resolution and non-ionizing characteristic.<sup>1,2</sup> Incoherent imaging schemes or passive imaging systems inherently exhibit a low image contrast and poor resolution. Active imaging systems with multi-static multiple-input and multiple-output (MIMO) array have been gaining significant attention due to potential real-time imaging capabilities that can be realized with fast electronic switches/scanning. Such kind of MIMO imaging systems use a coherent synthetic aperture focusing technique, which usually uses sampling spacing on the order of  $\lambda/2$  in traditional uniform array to avoid aliasing. However, this dense sampling requirement increases the system cost dramatically when operating at mm-wave/THz bands because a large number of transceivers is required to achieve a wide Field of view (FOV). This limits the practical implementation of mm-wave/THz imaging systems, particularly electrically large systems for personnel screening. For example, a linear personnel screening system working at low mm-wave band of 24.25-30 GHz already uses 384 transmitter (Tx) antennas and 384 receiver (Rx) antennas in two linear uniform arrays.<sup>3</sup> A flat 2D array operating at 72-80 GHz consists of 3072 Tx and 3072 Rx elements.<sup>1</sup> Alternatively, we proposed linear sparse periodic arrays with the large element spacing to reduce the number of transceivers and data size, working ideally on imaging pure metallic targets with small holes.<sup>4</sup> However, this method will reduce the image signal-to-noise ratio (SNR) in certain extent, degrading its capability of detecting complex or challenging targets. To balance this conflict, the multi-pass (interferometric) synthetic aperture imaging has been proposed.<sup>5</sup> Regardless of the single-pass or multi-pass architecture for synthetic aperture imaging, fast integral equation-based techniques such as inverse multipole method or generalised synthetic aperture focusing technique (GSAFT) are used in image reconstructions because of multi-static MIMO setup.<sup>5,6</sup> However, these

---

Further author information: (Send correspondence to Shaoqing Hu)  
E-mail: shaoqing.hu@brunel.ac.uk

reconstruction algorithms are computationally expensive and this issue becomes prominent with increasing data volume. Thus, Fast Fourier Transform (FFT) based techniques are desired for real-time imaging applications. Nevertheless, the multi-static MIMO topology makes it impossible to directly apply the FFT technique. Therefore, an FFT-based matched filtering algorithm compatible with multi-static MIMO scenario is proposed.<sup>7</sup> The image reconstruction time (for a scene of 200 mm × 200 mm) reduces significantly to 0.04 s so this technique has potential to provide real-time imaging.<sup>7</sup>

In addition, a new technique called random sparse imaging has recently been emerging to further save the system cost while maintaining high image quality. In this context, two popular reconstruction algorithms are based on compressive sensing (CS) and low rank matrix completion (LRMC).<sup>5</sup> However, the CS-based method is sensitive to noise and has basis-mismatch problem. LRMC technique is an alternative but superior technique to reconstruct the missing samples in the sparse sampling process. It has been applied in remote synthetic aperture radar (SAR) imaging, W-band 0.4m- SAR imaging for target detection,<sup>8</sup> and 220 GHz multi-pass synthetic aperture imaging for 1.4 m target detection.<sup>5</sup> Unlike compressive sensing (CS), LRMC and LRMR do not require a high computational cost. Different from LRMC, LRMR assumes a large matrix of measured data  $M = L + E_0$  where  $L$  is a low rank matrix and  $E_0$  is sparse noise/error matrix.  $L$  matrix is recovered from measured matrix  $M$  in traditional LRMR applications. We develop this method to make use of error matrix  $E_0$ . This significantly improves the capability of target detection. The sparse sampling is achieved by an aperiodic array that originates from linear sparse periodic array. The proposed design method is simple and verified successfully with achieved imaging results.

## 2. FUNDAMENTAL PRINCIPLE AND THEORY

### 2.1 Design of Aperiodic Array and Scanning Scheme

A linear sparse periodic array (SPA) consisting of  $Nt$  Tx and  $Nr$  Rx elements, as shown in Figure 1(a), has been proposed for THz imaging. This kind of array has a constant Tx & Rx element spacing, which can be different from each other. It is capable of achieving real-time imaging because of fast electronic scanning, which is a low-cost and alternative solution to a uniform dense array. Like electronic scanning of traditional uniform dense arrays, the Tx of SPA is sequentially switched on as well and when one is in on status, all the receivers will record the echo amplitudes and phases. The resultant virtual  $Nt \times Nr$  samples are illustrated in Figure 1(a), which is the middle position of each Tx-Rx combination. The random sparse sampling can be achieved by an aperiodic array which removes a few transmitter or receiver antenna elements in a SPA. For example, Figure 1(b) shows an aperiodic array and its corresponding virtual sampling data. It consists of 7 transmitters and 7 receivers, which results from a SPA of 8 Tx and 8 Rx elements with 1 Tx and 1 Rx removed. With different number of elements removed, various sparse sampling patterns and sampling ratios can be obtained. This design method can be extended to a planar aperiodic array design. The planar scanning of a target region of interest can be achieved either by a planar array or by the mechanical scanning/movement of a linear array along the other direction.

Figure 2(a) and Figure 2(b) illustrate the sparse imaging scheme with the proposed linear aperiodic array and a virtual sparse sampling pattern of random 6 Tx & 6 Rx elements in each linear aperiodic array. The white box indicates the sampled data while the grey box indicates the missing data that will be recovered by sparse imaging algorithm. In addition, N-pass datasets with a path shift  $ds$ , as shown in Figure 2(c), are phase correlated to reconstruct an improved N-pass synthetic aperture focusing image. Figure 2(d) shows a target of pure metallic plate in the experiment. The full SPA array consists of 8 Tx and 8 Rx elements, configured as shown in Figure 1(a). In this setup, the Tx element spacing is 6 mm and the Rx element spacing is 24 mm. The separation spacing between the Tx array and the Rx array is 181 mm. The peak gain of horn is about 23.81 dB at 220 GHz and the typical input power to the horn at 220 GHz is -13 dBm (0.05 mW). The target distance from the scanning plane of horn output aperture is 1.4 m. The mechanical scanning length along y-axis is 0.3 m.

### 2.2 Fast Imaging of Multi-static MIMO Sparse Sampling

The initial sparse sampling data acquired with the aperiodic sparse array is termed as  $S_0$ . It is part of sampling data with full linear sparse periodic array, which is approximated by  $S_1 \in C^{(N_t N_r) \times N_y}$ . Therefore,  $S_0$  and  $S_1$  are subject to the following condition:

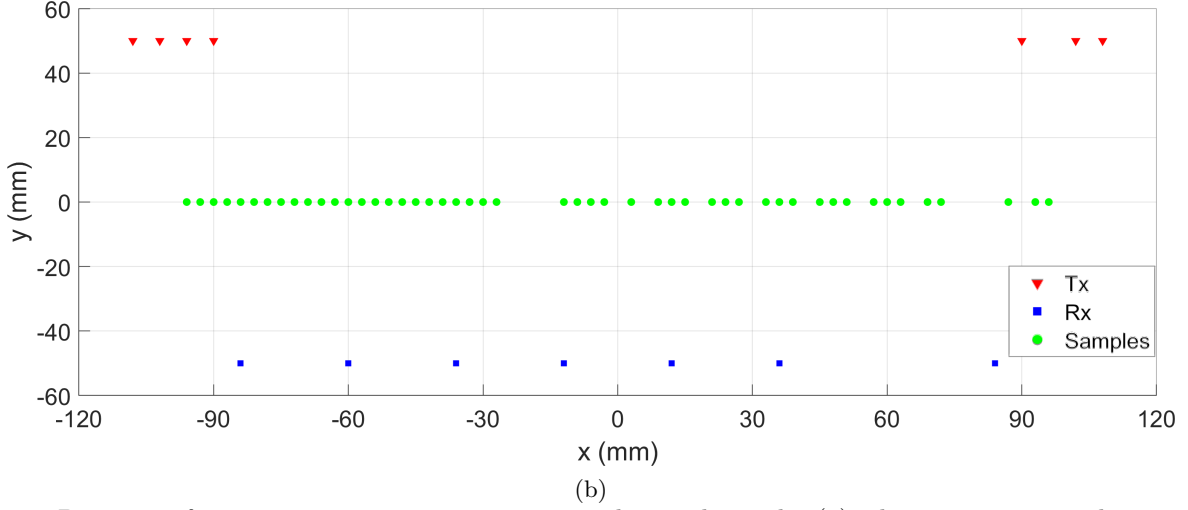
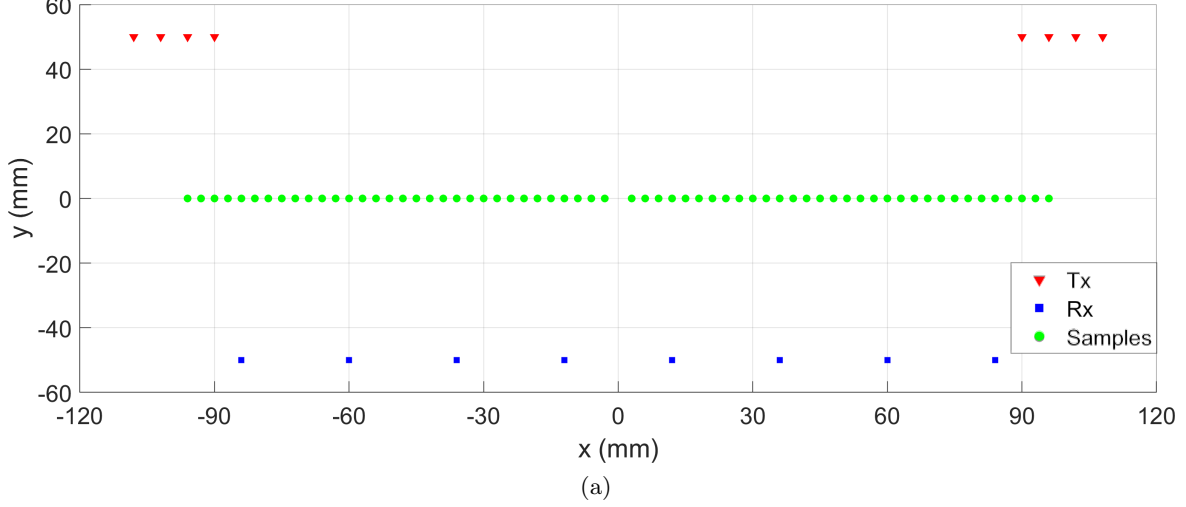


Figure 1: Positions of transmitter array, receiver array and virtual samples (a) a linear sparse periodic array (b) an aperiodic array of 7 Tx & 7 Rx elements.

$$S_0(i, j) = P_{\Omega_{sampled}} \cdot S_1 = \begin{cases} S_1(i, j), & (i, j) \in \Omega_{sampled}, \\ 0, & (i, j) \notin \Omega_{sampled}, \end{cases} \quad (1)$$

where  $P$  is a sparse sampling matrix consisting of 0 (white) and 1 (grey). The missing data in  $S_1$  can be recovered by solving the following nuclear norm minimization optimization problem:

$$\begin{aligned} & \text{minimize} \quad \|L_s\|_* + \lambda_s \|S_\epsilon\|_1, \\ & \text{subject to} \quad P_{\Omega_{sampled}} \cdot (L_s + S_\epsilon) = S_0, \end{aligned} \quad (2)$$

where  $\lambda_s$  is a scalar.  $\|L_s\|_*$  is the nuclear norm of component matrix  $L_s \in \mathbb{C}^{(N_t N_r) \times N_y}$ ,  $\|S_\epsilon\|_1$  refers to the  $l_1$ -norm of sparse error matrix and  $S_1 = L_s + S_\epsilon$ . Principal component pursuit by alternating directions method (PCPADM) is used to solve (2).<sup>9</sup>

Once the echo data, such as  $S_1$ , is obtained, a synthetic aperture focusing-based algorithm can be used to reconstruct the target image. The GSAFT algorithm is applicable to any MIMO topology but the reconstruction time increases with data volume. Using the GSAFT algorithm, it is impossible to achieve fast imaging of a large region of interest or at high frequencies like THz. The promising solution can be Fast Fourier Transform-based

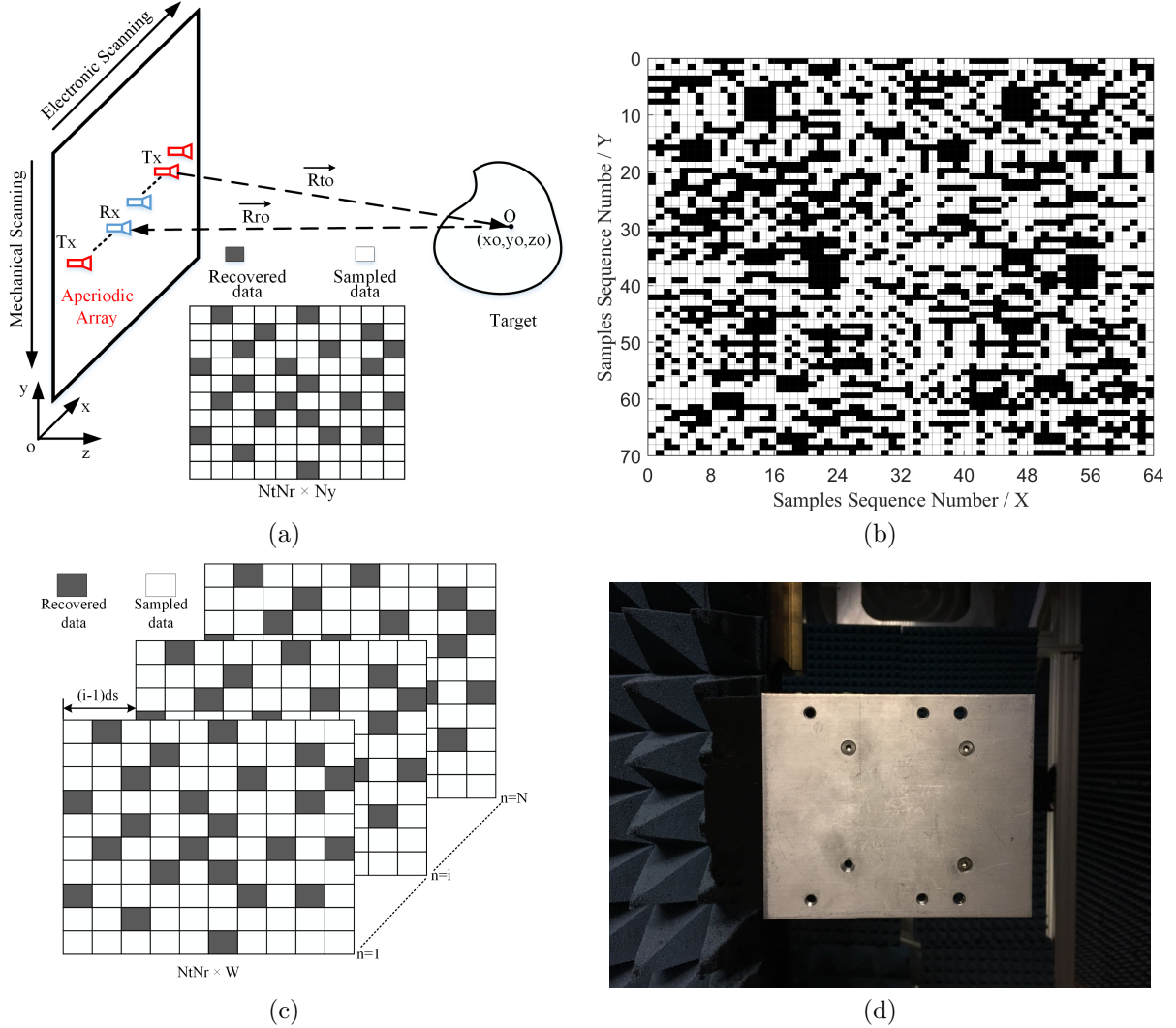


Figure 2: (a) Sparse imaging scheme (b) virtual sparse sampling pattern (6 Tx & 6 Rx elements in each aperiodic array) (c) multi-pass interferometric synthetic aperture sparse imaging (d) photo of metallic target under test.

image reconstruction techniques but such techniques can not be directly applied to  $S_1$  because of the multi-static multiple-input and multiple-output sampling scenario. Thus a multi-static to mono-static conversion is required to obtain a mono-static approximation matrix referred to as  $\tilde{S}_1$ .<sup>10</sup> After that, as shown in Figure 1(a), there is a sample missed in full SPA sampling data. It causes a gap and non-uniform spacing of virtual samples, so zero padding is required on  $\tilde{S}_1$ , resulting in  $\tilde{S}_2 \in C^{(N_t N_r + 1) \times N_y}$ .<sup>10</sup> Finally, when the large spacing in virtual samples is used, as 3 mm ( $2.20\lambda$ ) in x-axis and 4 mm ( $2.93\lambda$ ) in y-axis, it is demonstrated that additional zero padding within entries of  $\tilde{S}_2$  can be helpful to improve the image quality of FFT-based image reconstruction.<sup>7</sup> Thereafter, denser data referred to as  $\hat{S}$  is obtained and Fast Fourier Transform matched filtering approach (FFTMF) is used to reconstruct the image from  $\hat{S}$ . We propose to develop traditional FFTMF integrated with multi-pass scanning data.

### 3. EXPERIMENTAL IMAGING RESULTS

In the experiment of imaging a pure metallic target of Figure 2(d), the virtual sampling spacing in x-axis and y-axis are 3 mm and 4 mm, respectively. Three zeros are added between each sample, this leads to 0.75 mm

and 1 mm spacing in  $\hat{S}$ . Figure 3(a) shows the single-pass synthetic aperture focusing image reconstructed with full SPA sampling data and FFTMF approach. In comparison, Figure 3(b) shows the 4-pass synthetic aperture focusing image reconstructed with full SPA sampling data and FFTMF approach. The improved image quality after utilizing multi-pass scanning data is evident, which is equivalent to the most accurate reconstructions based on generalized synthetic aperture focusing technique. However, the reconstruction time is much reduced. The reconstruction time are reported to be 0.04 s for Figure 3(a) and 0.17 s for Figure 3(b). The execution of the algorithm was carried out on MATLAB running on a machine with Windows 10 Enterprise, Intel Core I7-10700 and random access memory of 16 G. The achieved practical resolution is about 6 mm at 1.4 m in both circumstances. In addition, Figure 3(c) and Figure 3(d) show the 4-pass synthetic aperture focusing images reconstructed by the FFTMF approach and with an aperiodic array of 6 Tx & 6 Rx elements and 7 Tx & 7 Rx elements, respectively. It can be seen that the practical resolution is maintained in sparse imaging and all the holes are still identifiable. Because of less missing data, Figure 3(d) shows superior image quality closer to Figure 3(b). It is worth noting that the spacing in fully recovered data  $S_1$  in x-axis and y-axis are 3 mm ( $2.20\lambda$ )

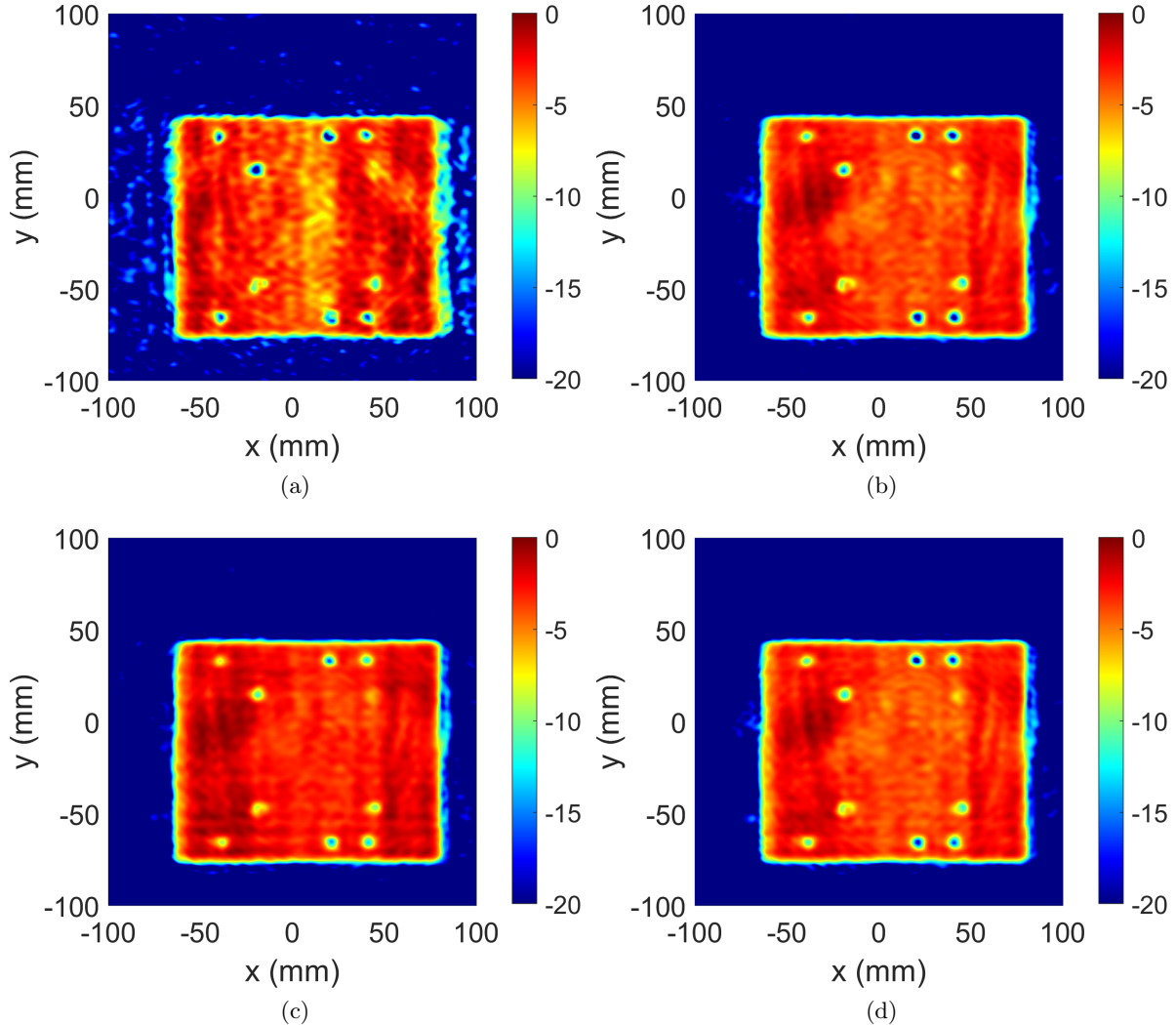


Figure 3: Reconstructed images of the metallic target under test using the FFTMF approach (a) single pass synthetic aperture imaging with full data (acquired by a SPA of 8 Tx & 8 Rx elements) (b) four-pass synthetic aperture imaging with full data (c) four-pass synthetic aperture sparse imaging with aperiodic arrays of 6 Tx & 6 Rx elements (d) four-pass synthetic aperture sparse imaging with aperiodic arrays of 7 Tx & 7 Rx elements.

and 4 mm ( $2.93\lambda$ ), which are consistent with its full SPA sampling but the amount of data is already much less than Nyquist sampling. Therefore, the achieved image quality is inspiring, especially using the simple and low-cost single-pass synthetic aperture focusing imaging like Figure 3(a).

Furthermore, imaging of an another, more challenging target has been tested. The target consists of a pattern of metallic patches etched on a substrate, as shown in Figure 4(a) in which the number indicates the width in millimeter. The coarse surface of substrate and low difference of permittivity between pattern and substrate make this target more difficult to be recognised than pure metallic plate. The virtual sampling spacing in x-axis and y-axis are 3 mm and 2.5 mm, respectively. Three zeros are added between each sample, this leads to 0.75 mm and 0.625 mm spacing in  $\hat{S}$ . The corresponding 3-pass synthetic aperture focusing image reconstructed by FFTMF approach with 6 Tx & 6 Rx elements is shown in Figure 4(b). It shows equivalent image quality of sparse imaging based on low rank matrix completion technique with single value thresholding (SVT) method.<sup>5</sup> Aforementioned sparse imaging based on LRMR technique uses  $L_s + S_\epsilon$  for image reconstruction. It is found that  $S_\epsilon$  only can be used for image reconstruction following the proposed procedures. This image provides complementary features of the target for identification.

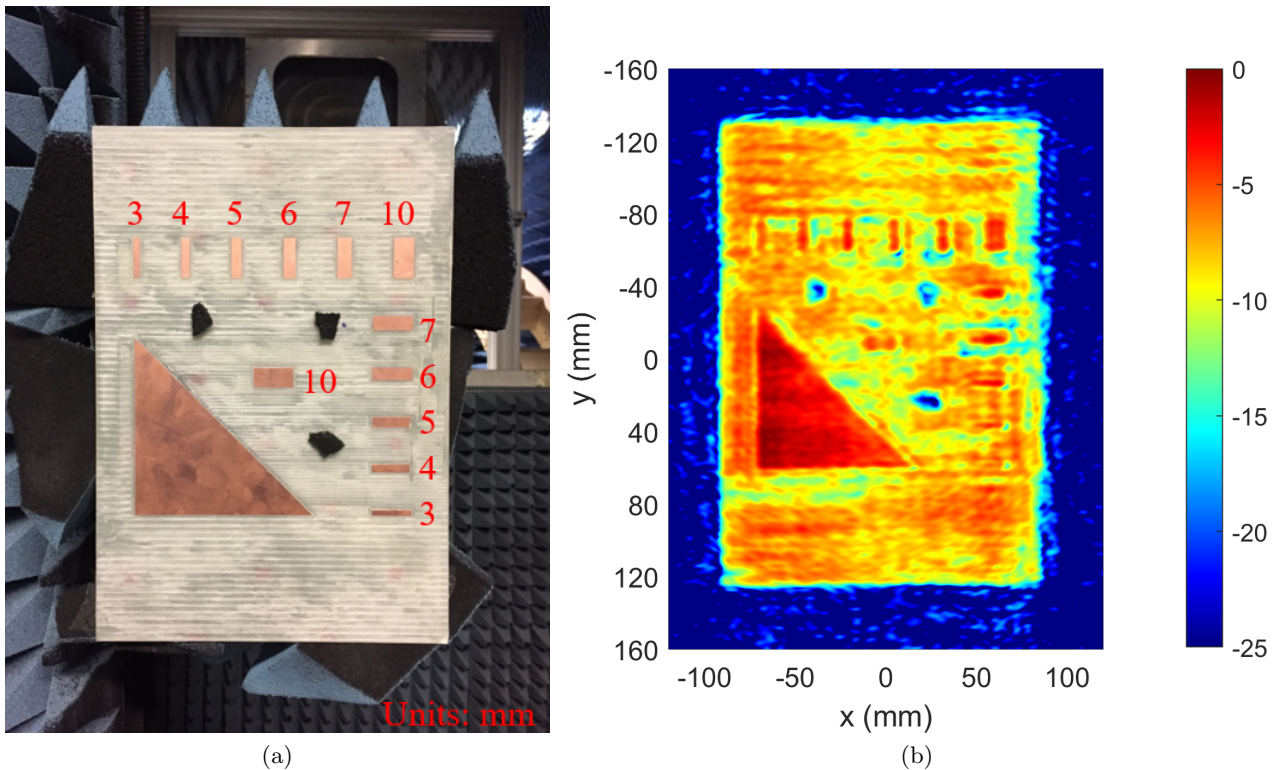


Figure 4: (a) Photo of challenging target under test with metallic pattern etched on dielectric substrate (b) reconstructed 3-pass synthetic aperture sparse imaging with the FFTMF approach and 6 Tx & 6 Rx elements.

#### 4. CONCLUSIONS

The design method of aperiodic sparse array resulting from linear sparse periodic array has been proposed for 220 GHz sparse imaging application. The corresponding sparse imaging algorithm based on low rank matrix recovery technique and improved FFT matched filtering technique has been proposed for fast image reconstruction. The proposed sparse imaging scheme has been experimentally verified successful. As part of the experimental campaign, two kinds of targets have been tested and 6 mm resolution at 1.4 m is achieved. The presented system can achieve 3D imaging with wideband operation, and it has potential to achieve real-time frame rates with proper system design.

## ACKNOWLEDGMENTS

The work is supported by Research Development Fund of Brunel University London under Grant LBG194.

## REFERENCES

- [1] Ahmed, S. S., Schiessl, A., Gumbmann, F., Tiebout, M., Methfessel, S., and Schmidt, L.-P., “Advanced microwave imaging,” *IEEE Microwave Magazine* **13**(6), 26–43 (2012).
- [2] Ahmed, S. S., “Microwave imaging in security — two decades of innovation,” *IEEE Journal of Microwaves* **1**(1), 191–201 (2021).
- [3] Sheen, D., McMakin, D., and Hall, T., “Near-field three-dimensional radar imaging techniques and applications,” *Applied Optics* **49**(19), E83–E93 (2010).
- [4] Hu, S., Zhou, M., Chen, X., and Alfadhil, Y., “Suppressing ghost images for synthetic aperture THz imaging with large sampling spacing,” in [12th European Conference on Antennas and Propagation (EuCAP 2018)], (2018).
- [5] Hu, S., Shu, C., Alfadhil, Y., and Chen, X., “Advanced thz mimo sparse imaging scheme using multipass synthetic aperture focusing and low-rank matrix completion techniques,” *IEEE Trans. Microw. Theory Tech.* **70**, 659–669 (Jan. 2021).
- [6] Gonzalez-Valdes, B., Alvarez, Y., Mantzavinos, S., Rappaport, C. M., Las-Heras, F., and Martinez-Lorenzo, J. A., “Improving security screening: A comparison of multistatic radar configurations for human body imaging,” *IEEE Antennas and Propagation Magazine* **58**(4), 35–47 (2016).
- [7] Hu, S., Molaei, A. M., and Yurduseven, O., “Reconstruction techniques for sparse multistatic linear array microwave imaging,” in [2022 17th International Workshop on Antenna Technology], (May 2022).
- [8] Wu, S., Ding, L., Li, P., Li, Y., Chen, L., and Zhu, Y., “Millimeter-wave sar sparse imaging with 2-d spatially pseudorandom spiral-sampling pattern,” *IEEE Trans. Microw. Theory Tech.* **68**, 4672–4683 (Nov. 2020).
- [9] Candès, E. J., Li, X., Ma, Y., and Wright, J., “Robust principal component analysis?,” *J. ACM* **58**, 1–37 (May 2011).
- [10] Molaei, A. M., Hu, S., Skouroliahou, V., Fusco, V., Chen, X., and Yurduseven, O., “Fast processing approach for near-field terahertz imaging with linear sparse periodic array,” *IEEE Sensors J.* **22**(5), 4410–4424 (2022).